Materials Science Forum
ISSN: 1662-9752, Vol. 1130, pp 13-23
doi:10.4028/p-Sx9Jhd

Submitted: 2023-11-21
Revised: 2024-03-13
Accepted: 2024-03-18
Online: 2024-10-31

Optimization of Geometric Design of Extruded Products Incorporating Properties, Cost and CO_2 Footprint

Anders Nesse[1,a*], Mads Iddberg[2,b], Ole Runar Myhr[3,4,c], Trond Furu[5,6,d]

[1]Hydro Extrusions, Drammensveien 264, Oslo, Norway, anders.nesse@hydro.com

[2]SINTEF Manufacturing, Grøndalsvegen 2, Raufoss, Norway, mads.iddberg@sintef.no

[3]Hydro Aluminium R&D, Romsdalsvegen 1, Sunndalsøra, Norway, ole.runar.myhr@hydro.com

[4]Norwegian University of Science and Technology, Department of Structural Engineering, Richard Birkelands vei 1A, Trondheim, Norway

[5]Norsk Hydro, Corporate Technology Office, Drammensveien 264, Oslo, Norway, trond.furu@hydro.com

[6]Norwegian University of Science and Technology, Department of Material Science and Engineering, Alfred Getz vei 2, Trondheim, Norway

[a]anders.nesse@hydro.com, [b]mads.iddberg@sintef.no, [c]ole.runar.myhr@hyodr.com, [d]trond.furu@hydro.com

Keywords: Extrusion, design, optimization, simulation, CO_2

Abstract. In this paper, a numerical simulation methodology has been applied to optimize the design of extruded aluminium products. The methodology, PRO^3 ^{TM}, incorporates product properties, production- and material costs as well as CO_2 footprint in an optimisation procedure. This allows for multi-objective optimisation and avoids sub-optimisation of for instance properties on the expense of production costs or CO_2 emissions. The outcome that follows from this multi-objective optimisation procedure, is that the resulting profile cross section will be different when the optimisation is based solely on property considerations, than when costs, and CO_2 emissions are introduced in the optimisation procedure.

The present methodology requires that the main processes and operations along the aluminium process chain are represented by physics based, predictive models of various types, including material- and mechanical models, in addition to cost-, and sustainability models. A standard multi-objective optimization algorithm is used to combine the models and for automatic running through-process simulations in iterations.

In this article, the PRO^3 ^{TM} methodology has been applied for optimisation of the profile cross section in case-studies with various user requirements. It has been demonstrated that the resulting cross section geometry depends on the specified relative importance of conflicting requirements like the desire for high productivity on the one hand, and the desire for low material costs and low CO_2 emissions on the other.

Introduction

To compete in a wide range of market segments, the aluminium industry must meet the customer requirements in terms of product quality, consistency, and price. In addition, sustainability and low carbon products are now becoming increasingly important for consumers, producers, and legislators. The complexity of balancing these opposing product requirements is proposed solvable with a holistic modelling tool, PRO^3 ^{TM} [1-3]. With respect to the CO_2-emission, each process and operation along the aluminium production chain, from bauxite and alumina to the finished extruded profile, must be taken into consideration. The use of end-of-life aluminium products becomes more and more attractive as a metal source as there is a 95% reduction of energy consumed compared to primary based metal [4]. A metal charge consisting of significant amounts of post-consumer scrap (PCS) may have a wider chemical composition window than primary based metal depending on the scrap type

and the available sorting methodologies. Consequently, high levels of PCS may affect both the thermomechanical treatment along the value chain and the properties of the product.

The cost of an aluminium product depends on the weight of the extruded profile. The present article demonstrates that the optimum profile design for a given product can be influenced by the amount of PCS used, as the mechanical properties may vary due to the larger chemical composition window. This article does not consider the design of the profile itself, nor does it employ the use of meta-models, such as other articles have [5-11]. It instead relies solely on physics-based and finite element modelling. While previously, PRO$^{3\ TM}$ has been used to optimize processing parameters, similarly to other authors [12], the current article focuses on the design of the profile.

A supplier and its customers of aluminium products are always searching for the best possible compromise in relevant properties, weight, processability and the CO_2-footprint of the product. The PRO$^{3\ TM}$-methodology has the potential to propose the optimal compromise.

The work presented in this article takes the established PRO$^{3\ TM}$ [1-3] concept to a new level. In addition to a holistic consideration of the process chain and the use of an optimization engine, the methodology is used for design of the product and analyse its performance in a digital environment like a digital twin. In sum, the tool can offer a strong compromise between processability, performance, and environmental impact.

Modelling Methodology

PRO^{3} TM. The present work is based on the PRO$^{3\ TM}$ concept – *Profit generation through Product and Process Optimization* – a digital twin of the product and its manufacturing process throughout the value chain – from casting to final properties. The backbone of PRO$^{3\ TM}$ consists of predictive, physics-based microstructure models on different length scales from nanometers to micrometers. combined with macro models (e.g., Finite Element Models) describing the industrial process of interest. The sophistication and complexity of each model varies from basic to cutting edge. Python has been used as an orchestration tool, responsible for facilitating the simulations, transferring data between models, and allowing the optimization software to control the process- and design parameters.

With reference to Fig. 1, each simulation starts with a selection of inputs chosen by the optimization tool. For this instance, the algorithm chooses a profile cross section design within predefined boundaries, and a recycled scrap content from 0 to 100 %. The profile is constructed using a finite element tool, and the design and material are evaluated in a defined case study. If the design passes product requirements, the extrudability is evaluated as well as the CO_2 and costs of manufacture. The optimization algorithm is based on pymoo [13], an open-source multi-objective optimization tool.

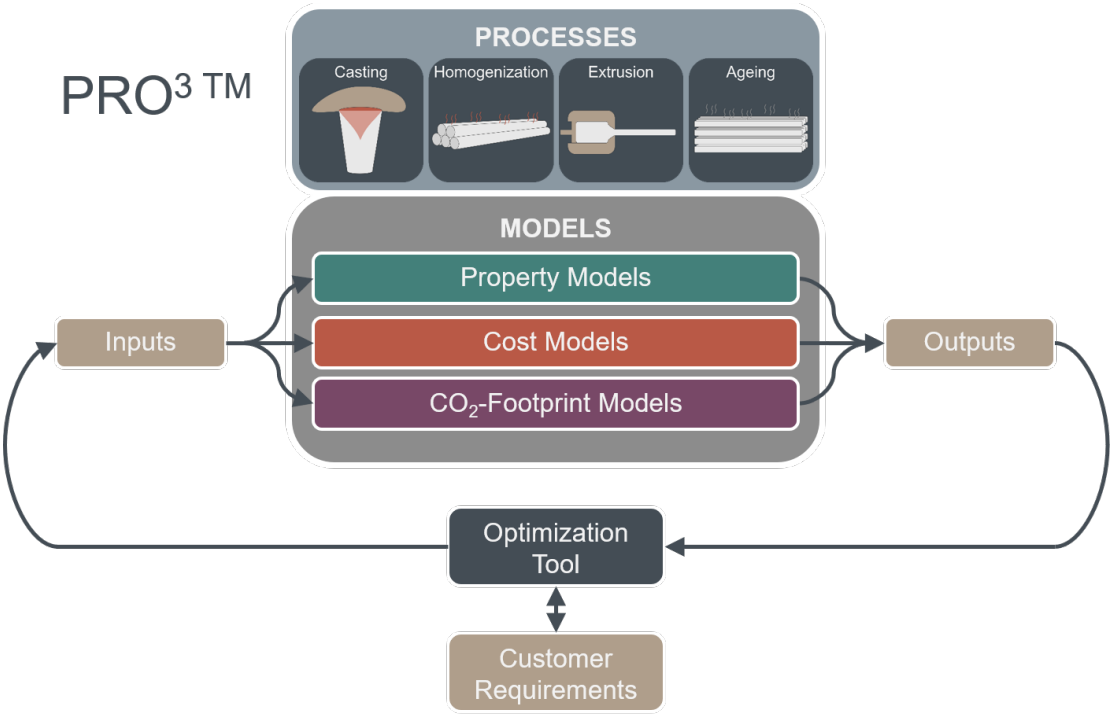

Fig. 1. PRO$^{3\ TM}$ schematic diagram [1-3]. PRO$^{3\ TM}$ contains a variety of different models, each describing a process or phenomenon along the aluminium process chain from casting to finished product. The simulations are orchestrated by a Python framework, and the in- and outputs are governed by an optimization tool based on the open-source optimization package pymoo.

Models

Each of the applied models are explained in short in the following section. For a detailed description of each model, the reader is referred to dedicated articles.

FEM model. IMPETUS Afea Solver® [14] is a commercially available finite element code specialized in nonlinear explicit analysis. Here, IMPETUS is used as an evaluation tool for the crushing of a profile. It is suited due to its implementation of higher order elements, making it less prone to inaccuracies due to slightly distorted element geometries. The iteration loop in this study relies on autogenerating a new mesh for each new set of geometry parameters and the auto generation algorithms found in most FEM software is prone to produce badly shaped element for complex cross section unless manually controlled.

NaMo. NaMo is a combined precipitation, yield strength and work hardening model for 6xxx alloys. The model predicts the evolution of the precipitate structure during a non-isothermal heat treatment based on alloy composition. The relevant parameters from the precipitate module of NaMo are used to calculate the yield stress and the work hardening rate through dislocation mechanics, and a complete stress-strain curve at room temperature can be predicted. The model has been described in several publications, such as [15-17].

AlEx. This model is an analytical approach to extrusion simulation, suited for rapid evaluation of the maximum ram speed resulting in surface tearing [18]. The model takes alloy composition, homogenisation cycle, and profile geometry as input and estimates the maximum allowable ram speed before the onset of surface tearing for billet preheat temperatures between 400 and 540°C. To enable the analytical solution of the resulting exit temperature, the model relies on the assumption that the surface exit temperature can be estimated as a sum of individual temperature contributions, as given in Eq. (1):

$$T_S = T_0 + \sum_i \Delta T_i. \quad (1)$$

Here, T_0 is the initial billet temperature and ΔT_i are the individual heat contributions due to adiabatic heating, friction with the die and the container, heat conduction between the billet and the container, and additional redundant work. The contributions are described in detail in a separate paper to be presented at this conference [18].

Costs and Carbon Footprint. Concerning the production- and material costs and CO_2 expenditure, a simplified expression calculates these based on the recycled content and processing parameters. The total costs of an aluminium profile can be divided into three constituents as shown below:

$$C = C_m + C_p + C_l. \quad (2)$$

The contributions represent the cost of material (C_m), production (C_p), and logistics (C_l). For simplicity's sake, logistics is neglected in this article. C_m is calculated from the costs of primary metal and scrap. The production term C_p covers all aspects of manufacturing and can be further divided into two terms, one for fixed costs, and one for variable costs. The fixed costs are ignored in this case since they do not affect the optimisation. While not always the case, productivity of extruded products is often limited by the ram speed during extrusion. When compared to a reference case, what remains is a simplified expression for relative cost [2]:

$$\Delta C = \Delta C_m + k_E \left(\frac{1}{v_{ram}} - \frac{1}{v_{ram}^{ref}} \right). \quad (3)$$

Here, k_E represents the cost of operating an extrusion press. This term will vary between different sites depending on factors such as the fixed costs and costs of labour and energy. v_{ram} and v_{ram}^{ref} are the extrusion ram speed for the comparative case and for a reference case, respectively. If extrusion ram speed is measured as millimetres per second, the k_E term is measured in cost per second of operation.

From bauxite to anodizing – each process step for manufacturing of aluminium extrusions can be tied to some emission of CO_2. Here, we estimate the total amount of CO_2, M, in kg per kg of finished aluminium product as follows [2]:

$$M = M_E + M_C + M_R. \quad (4)$$

Here, the indices denote E – electrolysis, C – casting, R – rest. As with cost, the rest term is considered constant and therefore neglected such that only a relative CO_2 emission is considered. The remaining terms, M_E and M_C, depend on the fraction of electrolysis metal (F_E), the fraction of process scrap (F_{PS}) and the fraction of post-consumed scrap (F_{PCS}).

Through the electrolysis process, CO_2 is directly emitted when the carbon anode is consumed. Indirectly, CO_2 is also emitted in the consumption of energy – mainly electricity – which varies widely depending on the source. Hydroelectric being one of the least emissive, while coal power is among the most emissive. Furthermore, the remainder of the process chain will emit CO_2 either directly or indirectly through the consumption of energy. Simplifying this system into only electrolysis and recycled (post-consumed scrap) metal, the CO_2-index M can be expressed as follows [2]:

$$M = (1 - F_{PCS})(a + bQ_e + M_{rest}) + bQ_r F_{PCS}. \quad (5)$$

Here, a represents carbon emission of the electrolysis process, and b is the carbon emission of energy production. Q_e and Q_r are the energy expenditure of electrolysis and remelting, respectively.

M_{rest} is the carbon emission associated with other processing steps than electrolysis and casting. F_{PCS} is the fraction of post-consumer scrap. For the optimisation simulations presented in this paper, M is treated as a function of F_{PCS}, where the latter is chosen at the will of the optimisation algorithm with a value from 0 to 1 inclusive. Typical values for the parameters in Eq. (5) are listed in Table 1 [2].

Table 1. Parameters for CO_2 calculations [2].

	a [kg CO_2/ kg Al]	**b** [kg CO_2/ kWh]	**Q_e** [kWh/kg Al]	**Q_r** [kWh/kg Al]	**M_{rest}** [kg CO_2/ kg Al]
Value	1.7	0.005* 1.0**	13.0	0.65	3.6

* Hydroelectric [19].
** Coal [19].

Optimization Tool. The optimization algorithm used in these simulations is NSGA-II [20] – Non-dominated Sorting Genetic Algorithm – implemented in the open-source Python package pymoo. The algorithm is genetic with modified mating and survival selection. In simpler terms, the algorithm treats every set of inputs as an individual with the possibility of survival and mating based on the optimization criterion. The most fit inputs merge pairwise, while the least fit set of inputs are discarded.

Simulation, Results, and Discussion

This section details cases where PRO^3 ^{TM} has been applied to handle real and relevant challenges from the industry. After outlining the simulation sequence, the next important step is to set the upper and lower bounds of the input variables. A wide range increases the likelihood that the optimal solution is found, but also increases the convergence time of the optimization algorithm.

Alloy. In an effort to restrain the complexity of the present cases and to demonstrate the effect of alloy composition on product design, the candidate alloys have been narrowed down to one 6082-type of alloy where the iron content is varied between 0.05 wt%, and 1.0 wt% as shown in Table 2. Such a high Fe-content could result from a poorly sorted scrap pile with high levels of iron. This fictive recycled alloy – although unrealistic with the current standards of recycled aluminium – represents a more difficult type of scrap that is detrimental to the properties and processability that may become more common in the future. In the simulations, the algorithm can mix the primary and recycled material in any balance from 0 to 100 %.

Table 2. Alloy composition for a primary 6082-alloy with very low Fe-content, and a fictive recycled 6082 from a poorly sorted scrap pile with unusually high levels of iron.

	Si [wt%]	**Fe** [wt%]	**Cu** [wt%]	**Mn** [wt%]	**Mg** [wt%]	**Cr** [wt%]	**Al** [wt%]
Primary	0.98	0.05	0.025	0.48	0.64	0.015	bal.
Recycled	0.98	1.0	0.025	0.48	0.64	0.015	bal.

It must be emphasised that remelt plants usually hold several possible sorted and separated materials to choose from when producing extrusion billets, in addition to primary aluminium from the electrolysis process, and different types of master alloys.

The processing conditions assumed in the simulations corresponds to a typical thermo-mechanical process route for 6082 alloys used in the industry. In this instance, each alloy has been homogenised for 2.25 hours at 575 °C and extrudability was evaluated by comparing productivity on a rod shape for each given material. To estimate the strength, each alloy was subjected to a single step artificial ageing heat treatment at 185 °C. Simulation results from NaMo are shown in Fig. 2 for the 6082

variants in Table 2 at four different Fe-concentrations. Fig. 2 (a) shows the yield strength evolution during artificial ageing, while Fig. 2 (b) shows the resulting stress-strain curves at maximum (T6) strength.

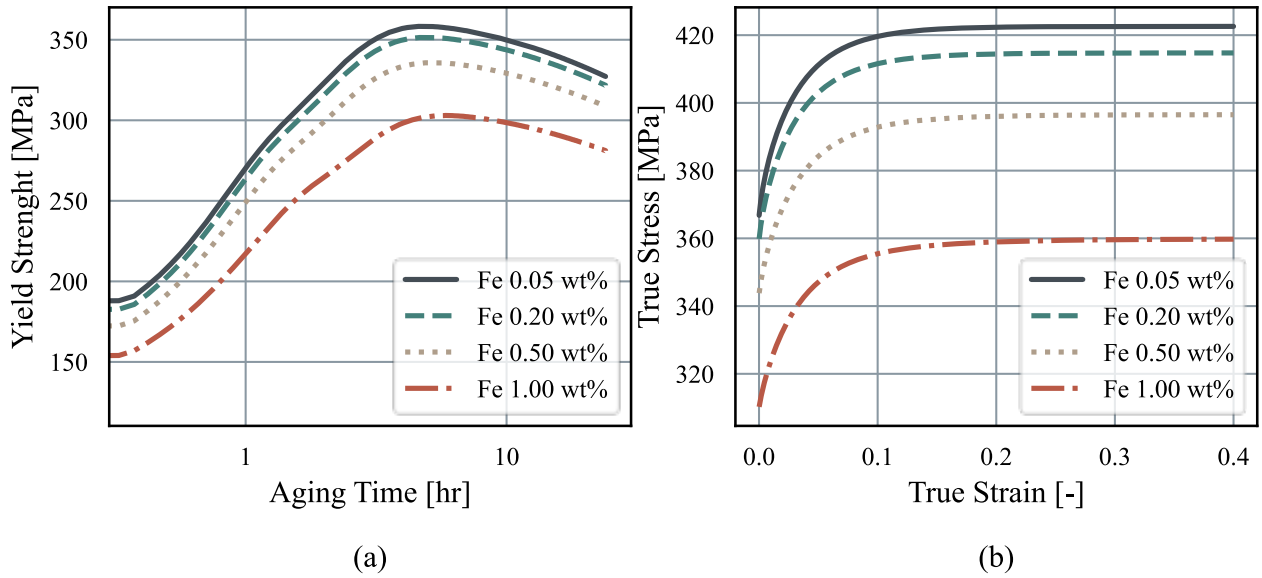

(a) (b)

Fig. 2. Results from NaMo simulations for a 6082-type of alloy with different Fe-content. (a) Yield stress curves during artificial ageing at 185 °C. (b) Stress-strain curves at peak strength.

As demonstrated in Fig. 2, iron has an increasingly detrimental effect on the strength of the material, especially above 0.5 wt%. The main effect of iron on the strength is that silicon is tied up in the Fe-rich phases that form during casting and homogenisation, reducing the available solid solution concentration of Si to form hardening Mg-Si type of particles during artificial ageing.

Load Case. A rear underrun protection device (RUPD), commonly made in steel or aluminium, is a safety measure meant to protect smaller vehicles in the event of a rear-end collision with a large vehicle. The load case presented is based on this automotive device.

Fig. 3 (a) shows a schematic illustration of the placement and function of a RUPD. In this work, the design considerations needed to fully design a functional RUPD profile will be simplified considerably, e.g., the fastening system is entirely neglected. The load scenario will be divided into two separate load cases, i.e., crush load and bend load. Both loads are considered quasi-static and are inspired by UN Regulations [21]. A schematic RUPD and the loads applied to the structure is shown in Fig. 3 (b).

- Crush load, F1: The RUPD is to withstand a crush load of 180 kN applied perpendicular to the profile length direction. The crush scenario is modelled with a finite element model as a short profile segment crushed between two rigid blocks. The profile is only allowed minor plastic deformation.
- Bend load, F2: The RUPD is assumed as an idealised cantilever beam in bending, subjected to the moment caused by a point force of 100 kN with a 500 mm lever arm. The load causing onset of plastic deformation in the cross section is assumed as the dimensional criteria.

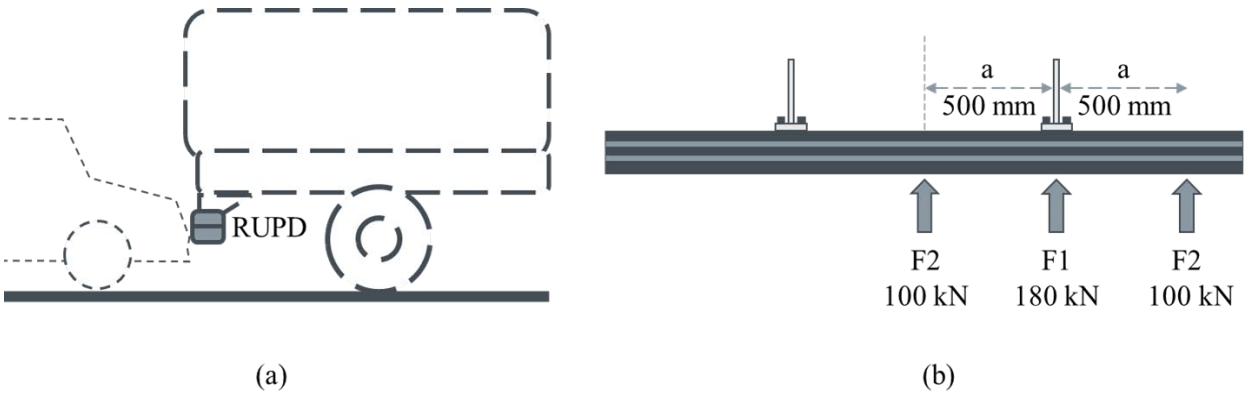

Fig. 3. Illustration of the function and load case for a rear under protection device (RUPD). (a) Schematic illustration of a RUPD meant to protect smaller vehicles in the event of a rear-end collision with a large vehicle. (b) Schematic illustration of RUPD and the loads applied to the structure.

Parameterised Geometry. In this work it was chosen to investigate a simple two-chamber profile, neglecting any details needed for assembly of the profile to the vehicle. A schematic of the profile is given in Fig. **4** (a), showing the orientation of the cross section of the profile relative to the load direction. The profile was parameterized assuming two planes of symmetry, allowing the wall thicknesses, the outer and inner radii, and a thickness transition area at the mid wall to vary. The outer contour of the profile was assumed to be square and fixed with side lengths of 140 mm. The double symmetric representation of the profile is given in Fig. **4** (b).

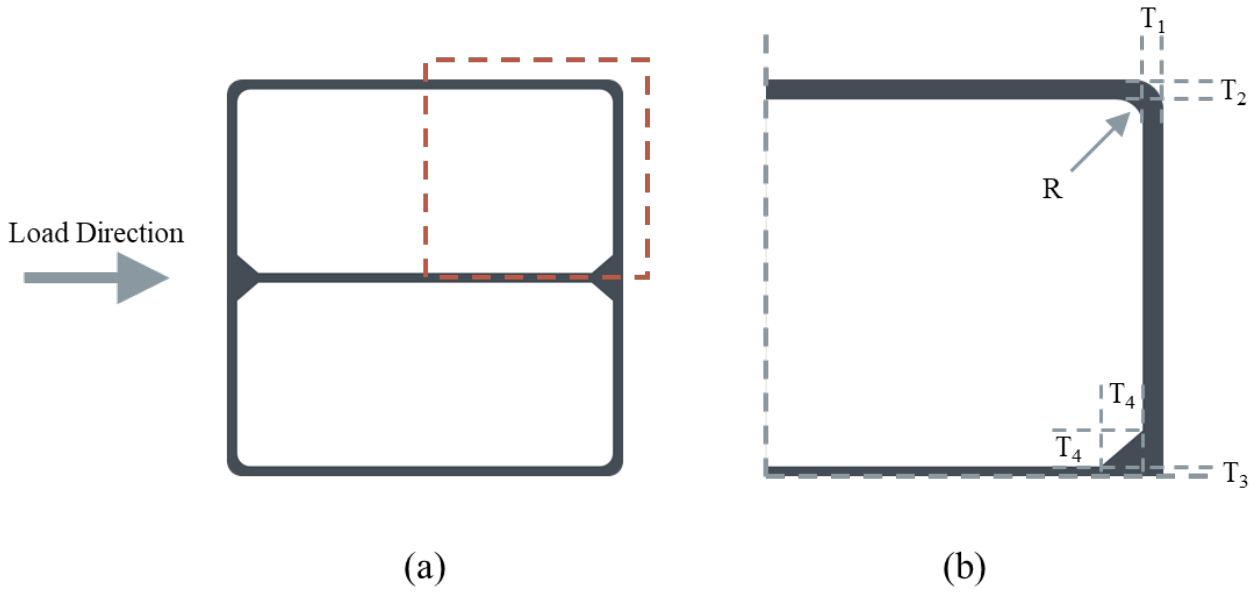

Fig. 4. (a) The full profile, illustrated in relation to the load direction. (b) Double symmetric representation of the RUPD profile, indication what parameters was allowed to vary.

In addition to the constraints imposed by the fixed outer geometry and the symmetry definition, each geometry parameter was given a range interwall. The allowable variance of each parameter is given in Table 3. The profile and parameterisation chosen is relatively simple to ease the effort of autogenerating a mesh for the profile. It is worth noting that the type of geometry representation chosen in this work considerably constrains the solution space explored by the optimisation algorithm. As the solution space only covers square double symmetric two-chamber profiles with a fixed outer geometry, it must be stated that the universally optimal profile for this type of application may not be found. Representation of geometry in optimization applications is a separate field of study and is beyond the scope of this work. The main motivation behind the chosen parameterisation was

to give the modelling framework a representative geometry representation to analyse and at the same time ensure that the geometry was easily meshed and handled by the other computational modules.

Table 3. Value range for variables in the parameterised geometry illustrated in Fig. 4 (b).

	T1 [mm]	T2 [mm]	T3 [mm]	T4 [mm]	R [mm]
Parameter bounds	2 – 8	2 – 8	1 – 4	1 – 10	2.5 – 20

Case Studies

Case 0 is the reference case, where only the geometry of the profile is optimized to both demonstrate a working framework and optimization algorithm, as well as establish a reference for comparison in the latter case.

The restrictions of the profile design are based on Fig. 4 and Table 3. Looking at the convergence plot in Fig. 5, it is evident that both optimisation runs converge towards a favourable light weight solution that satisfies the constraint equations defined by the minimum allowable bending and crush load. On average, the primary based alloy has a lower profile weight compared to the PCS-based alloy. The difference reflects the reduction in yield and flow stress as shown in Fig. 2 (b) when introducing a high iron content.

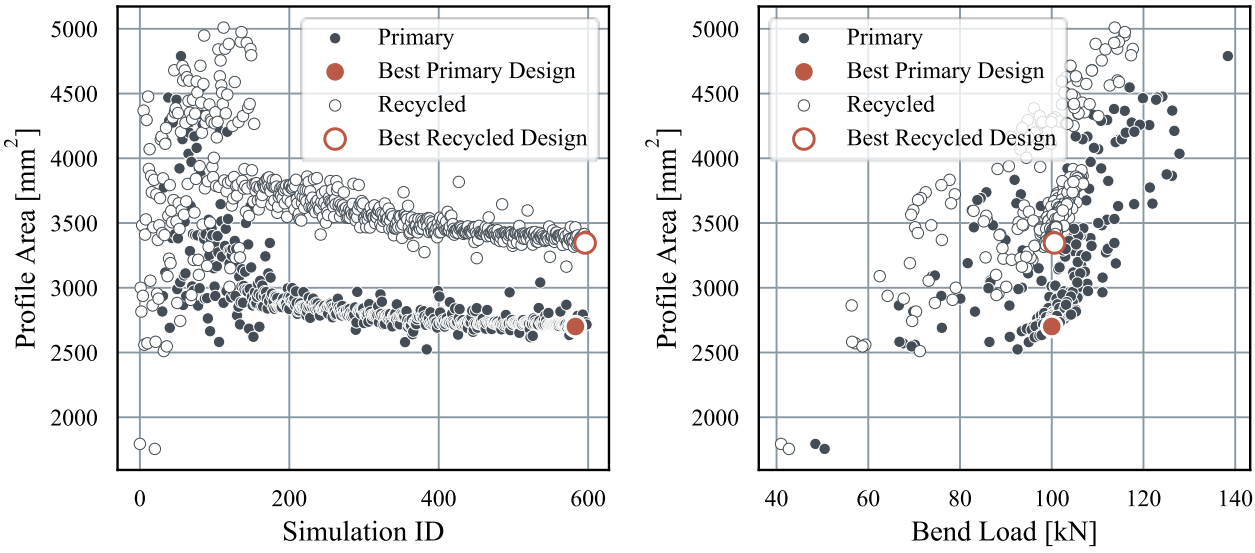

Fig. 5. Key results from PRO^3 ^{TM} Case 0 optimisation simulation. (a) shows how the simulations converge towards a lighter design for both primary and recycled material, while (b) shows the pareto fronts for bend load vs profile area.

Based on the simulation runs visualised in Fig. 5, one can identify the two most lightweight solutions that satisfies the load-based constraint equations. The two designs are shown in Fig. 6, where Fig. 6 (a) shows the lightest design with 100 % primary aluminium and Fig. 6 (b) shows the lightest design with 100 % recycled material. As one would expect the optimisation framework pushes the mass of the profiles as far away from the neutral axis of the profile as possible to maximize the second area moment of the profiles to satisfy the demand on bending load. Given the parameterisation chosen in this demonstration case, the algorithm must add additional mass in the corner section of the mid-wall to satisfy the load constraint for the simulation run with recycled aluminium due to the lower strength of the material.

	T1 [mm]	T2 [mm]	T3 [mm]	T4 [mm]	R [mm]
#583-1	6.8	2.0	1.0	3.1	3.8
#596-2	7.7	2.0	2.0	9.5	3.5

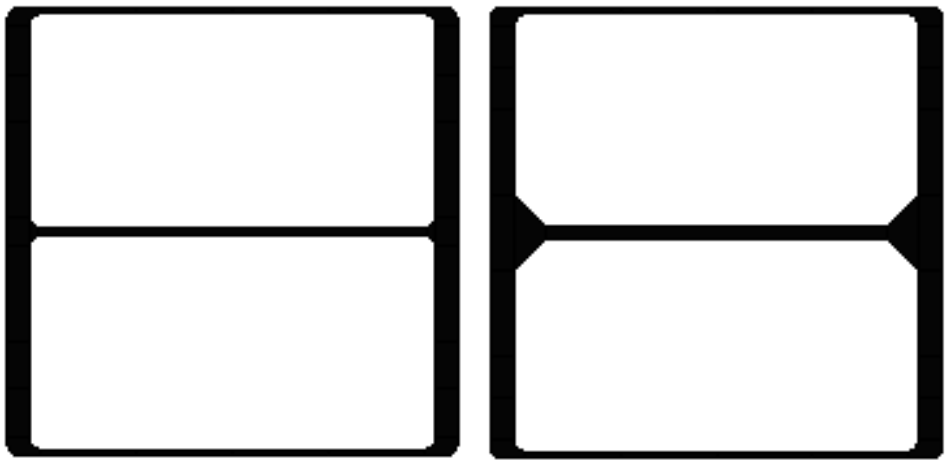

(a) (b)

Fig. 6. Resulting profile designs comparing the two edge cases of primary and recycled material. (a) 100% primary material, simulation #583-1. (b) 100% recycled material, simulation #596-2.

Case 1 builds upon Case 0 and introduces the importance of production costs, material costs and CO_2 footprint. When designing profiles, it may be tempting to create the most topologically optimized unit. However, if this design is difficult to extrude, the savings from lightweighting can be cancelled out by lower productivity, or vice versa. In this case, the profile simulated in Case 0, #583-1 from Fig. 6 (a) is used as a reference design for comparison.

In the setup for the simulations, the following parameters were minimized by the algorithm: CO_2-, material-, and production costs – while also maintaining the mechanical load requirements. Similar to Fig. 5 from Case 0, Fig. 7 shows the key results from Case 1. The two figures are very comparable, but an additional layer of complexity is added by having alloys with a continuous spectrum of primary and recycled content.

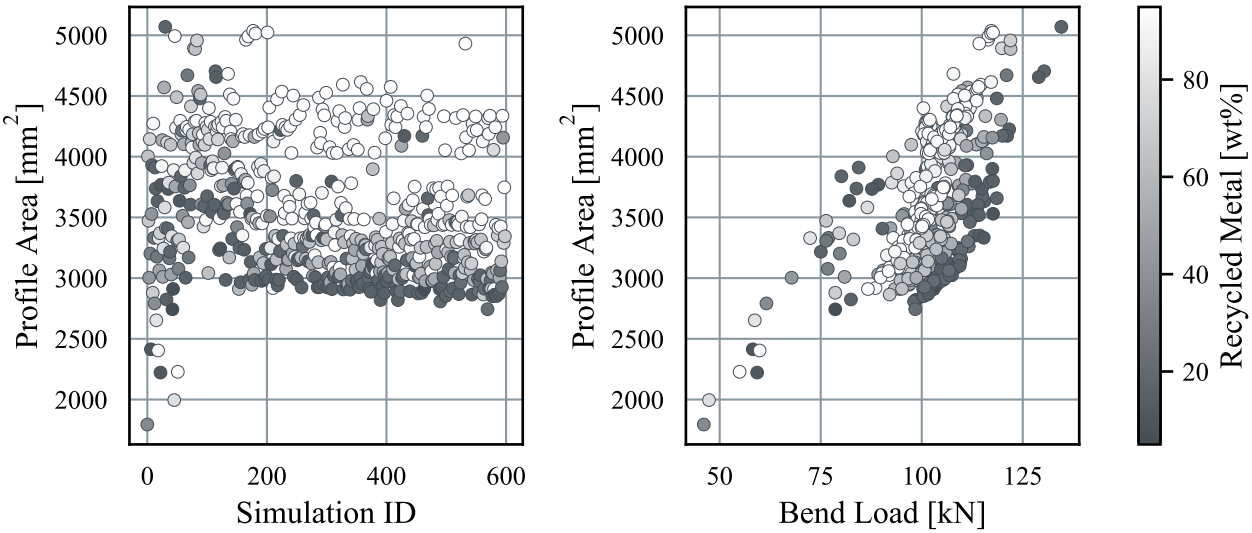

(a) (b)

Fig. 7. Key results from PRO^3 ™ Case 1 optimization simulation. (a) shows how the simulations converge towards a lighter design for different fractions of recycled metal, while (b) shows the pareto fronts for bend load vs profile area.

This extra dimension allows customers and manufacturers to make a smarter selection when encountering strict demands. E.g., for the automotive industry, this analysis would allow for a better compromise between unit weight and carbon footprint. Perhaps choosing a design that is lighter than #596-2, but more environmentally friendly than #583-1, both from Case 0.

The optimisation parameters are illustrated in Fig. 8, where manufacturing- material-, carbon and total monetary cost is illustrated.

From Fig. 8 (a), it is shown that the profile exit speed is comparable for all balances between primary and recycled metal. On one hand, for a given extrusion ram speed, the smaller cross section profile will extrude faster than a larger cross section profile, taking into account of the difference in reduction ratios. On the other hand, the models prefer to extrude high iron content alloy due to the lower deformation resistance, as evidenced by Fig. 2. The two effects seem to cancel each other out.

From Fig. 8 (b), it is shown that it is possible to be competitive on cost while also delivering a lightweight and low carbon product, indicated by the leftmost markers. While the recycled material is in this instance cheaper to purchase, the corresponding profiles are bigger, leading to more material spent.

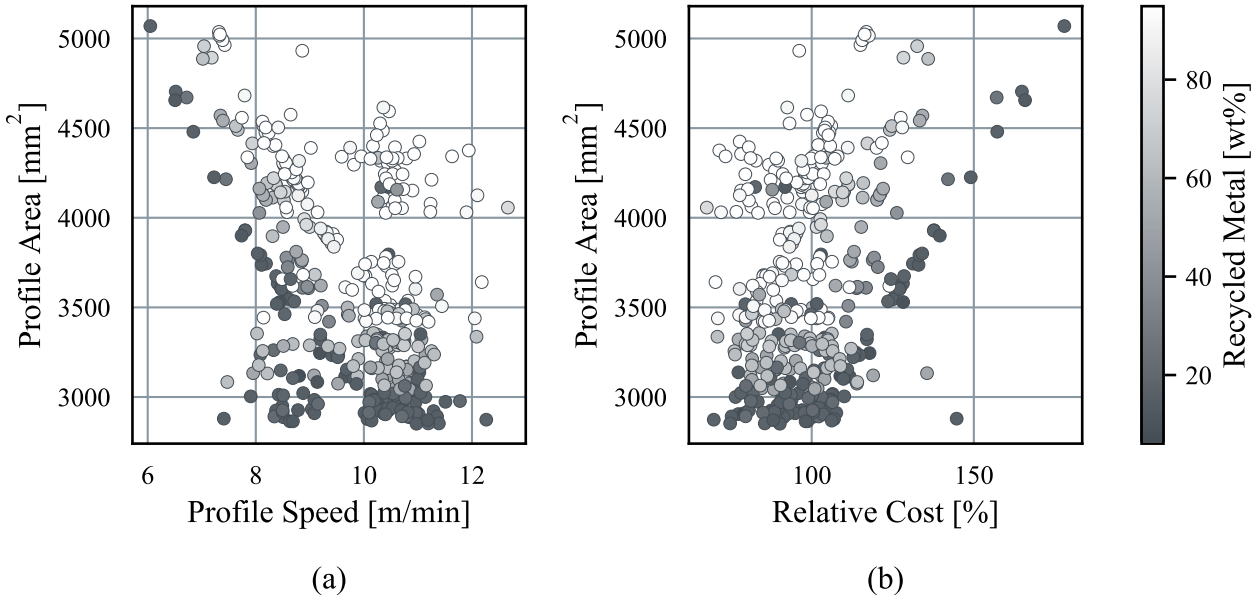

Fig. 8. Illustration of the main optimization parameters from the PRO^3 ^{TM} Case 1 optimisation simulation. Designs that did not meet the load requirements has been omitted. (a) shows the profile extrusion speed vs profile area. (b) shows the relative cost (compared to the best design from Case 0) vs profile area.

Concluding Remarks

This paper describes a holistic approach to optimisation of product properties, production costs and CO_2 footprint by using a simulation methodology called PRO^3 ^{TM}. The case studies in the present article are related to production of an automotive component based on 6xxx series aluminium extrusions with given functional requirements on crush- and bend loads. At the same time, CO_2 footprint and extrusion costs were attempted minimised. These examples illustrate how optimisation can be used by a product developer to estimate the effects of changes of the profile geometry profile before they are made.

The PRO^3 ^{TM} software is relevant for all levels in the organization. From the operator responsible for setting the extrusion recipe, to the salesperson giving quotes on products, and the strategic planners who decide on which alloys a plant should carry. Decision makers could decide on the right compromise between robustness of the mechanical performance of the product versus the emissions.

References

[1] T. Furu and O. R. Myhr, "Method for the Optimization of Product Properties and Production Cost of Industrial Process," (2014).

[2] O. R. Myhr, R. Østhus, J. Søreide and T. Furu, "A Novel Methodology for Optimization of Properties, Cost and Sustainability of Aluminium Extrusions," in *ET2016*, Orlando, (2016).

[3] T. Furu, R. Østhus and O. R. Myhr, "A Digital Twin for Production of Aluminium Extrusions," in *ET2020*, Orlando, (2022).

[4] Hydro, "Aluminium Recycling," [Online]. Available: https://www.hydro.com/en-NO/aluminium/about-aluminium/aluminium-recycling/.

[5] B. Reggiani, L. Donati and L. Tomesani, "Multi-goal optimization of industrial extrusion dies by means of meta-models," *The International Journal of Advanced Manufacturing Technology,* vol. 88, 2017.

[6] R. Pelaccia, M. Negozio and B. D. L. Reggiani, "Assessment of the Optimization Strategy for Nitrogen Cooling Channel Design in Extrusion Dies," *Key Engineering Materials,* vol. 926, 2022.

[7] G. Zhao, H. Chen, C. Zhang and Y. Guan, "Multiobjective optimization design of porthole extrusion die using Pareto-based genetic," *The International Journal of Advanced Manufacturing Technology,* vol. 69, 2013.

[8] N. Lebaal, F. Schmidt and S. Puissant, "Design and optimization of three-dimensional extrusion dies, using constraint optimization algorithm," *Finite Element in Analysis and Design,* vol. 45, no. 5, pp. 333-340, 2009.

[9] Z. Lin, X. Juchen, W. Xinyun and H. Guoan, "Optimization of die profile for improving die life in the hot extrusion process," *Journal of Materials Processing Technology,* vol. 142, pp. 659-664, 2003.

[10] S. T. Wang, R. S. Lee, H. Y. Li and C. H. Chen, "Optimal Die Design for Three-Dimensional Porthole Extrusion Using the Taguchi Method," *IMechE,* vol. 220, pp. 1005-1009, 2006.

[11] F. Gagliardi, G. Ambrogio, C. Ciancio and L. Filice, "Metamodeling technique for designing reengineered processes by historical data," *Journal of Manufacturing Systems,* vol. 45, 2017.

[12] S. Jajimoggala, N. Murali Krishna and K. Syed, "Selection of optimal hot extrusion process parameters for AA6061using hybrid MCDM technique," *Materials Today: Proceedings,* vol. 18, pp. 278-290, 2019.

[13] J. Blank and K. Deb, "pymoo: Multi-Objective Optimization in Python," *doi: 10.1109/ACCESS.2020.2990567,* pp. 89497-89509, (2020).

[14] IMPETUS Afea Solver®, IMPETUS Afea AS.

[15] O. R. Myhr, Ø. Grong and C. Schäfer, *Metall. Mater. Trans A,* vol. 46A, p. 6018, (2015).

[16] O. R. Myhr, Ø. Grong and K. O. Pedersen, *Metall. Mater. Trans A,* vol. 41A, p. 2276, (2010).

[17] O. R. Myhr, O. S. Hoppestad and T. Børvik, *Metall. Mater. Trans A,* vol. 49A, p. 3592, (2018).

[18] M. Iddberg, O. R. Myhr, A. Nesse and T. Furu, A Modelling Framework for Rapid Evaluation of Speed Limiations of Aluminium Profiles, Aluminium 2000, (2023).

[19] Environmental Metrics Report, International Aluminium Institute, (2014).

[20] K. Deb, A. Pratap, S. Agarwal and T. Meyarivan, A fast and elitist multiobjective genetic algorithm: NSGA-II, IEEE Transactions on Evolutionary Computation, (2002).

[21] Addendum 57: UN Regulation No. 58.